Inhibiting mGluR5 activity by AFQ056/Mavoglurant rescues circuit-specific functional connectivity in Fmr1 knockout mice

NeuroImage 191 (2019) 392–402

Contents lists available at ScienceDirect

NeuroImage

journal homepage: www.elsevier.com/locate/neuroimage

Inhibiting mGluR5 activity by AFQ056/Mavoglurant rescues circuit-specific functional connectivity in Fmr1 knockout mice

Valerio Zerbi [a,c,*], Marija Markicevic [a], Fabrizio Gasparini [b], Aileen Schroeter [e], Markus Rudin [c,d,e], Nicole Wenderoth [a,c]

[a] Neural Control of Movement Lab, HEST, ETH Zürich, Winterthurerstrasse 190, 8057, Zurich, Switzerland
[b] Novartis Institutes for BioMedical Research, Neuroscience Research, 4002, Basel, Switzerland
[c] Neuroscience Center Zurich, University and ETH Zurich, Winterthurerstrasse 190, 8057, Zurich, Switzerland
[d] Institute of Pharmacology and Toxicology, University of Zurich, Winterthurerstrasse 190, 8057, Zurich, Switzerland
[e] Institute for Biomedical Engineering, University and ETH Zurich, Wolfgang-Pauli-Str. 27, 8093, Zurich, Switzerland

ARTICLE INFO

Keywords:
Fragile-X
FMR1
Autism
Brain connectivity
Resting-state functional MRI
mGluR5

ABSTRACT

Previous work has demonstrated that neuroimaging biomarkers which capture functional connectivity of the brain can be used to define a specific and robust endophenotype in *Fmr1*$^{-/y}$ mice, a well-established animal model of human Fragile-X Syndrome (FXS). However, it is currently unknown whether this macroscopic measure of brain connectivity is sufficiently sensitive to reliably detect changes caused by pharmacological interventions. Here we inhibited the activity of the metabotropic glutamate receptor-5 (mGluR5) using AFQ056/Mavoglurant, a drug that is assumed to normalize excitatory/inhibitory neural signaling imbalances in FXS. We employed resting-state-fMRI (rs-fMRI) and diffusion-weighted imaging (DWI) to test whether Mavoglurant re-established brain connectivity - at least partly - within some of the affected circuits in *Fmr1*$^{-/y}$ mice that are related to social behavior deficits. In line with previous findings, we observed that *Fmr1*$^{-/y}$ mice exhibited impaired social interaction, reduced connectivity in three main functional networks and altered network topology. At the group level, Mavoglurant did neither rescue abnormal social behavioral nor white matter abnormalities; however, for some, but not all of these circuits Mavoglurant had a genotype-specific effect of restoring functional connectivity. These results show that rs-fMRI connectivity is sufficiently sensitive to pick up system-level changes after the pharmacological inhibition of mGluR5 activity. However, our results also show that the effects of Mavoglurant are confined to specific networks suggesting that behavioral benefits might be restricted to narrow functional domains.

1. Introduction

Fragile-X syndrome (FXS) is a monogenic developmental disorder characterized by intellectual disabilities, physical abnormalities and epileptic seizures, which is additionally associated with a high incidences of behavior that meets the diagnostic criteria for autism spectrum disorder (ASD) (Glass, 1991). In FXS an abnormal methylation of the fragile-X mental retardation 1 (FMR1) gene leads to a complete or partial absence of fragile-X mental retardation protein (FMRP)(Pieretti et al., 1991), which is otherwise highly expressed in the brain and acts as translational repressor of signaling pathways at the level of the synapses (Willemsen et al., 2011). Several studies showed that the severity of intellectual and social disabilities correlate with FMR1 activity and FMRP levels (Dyer-Friedman et al., 2002; Loesch et al., 2004; Tassone et al., 1999). Low levels or absence of FMRP causes an excessive translation of several target mRNAs involved in multiple neuronal signaling pathways, including the group I metabotropic glutamate receptors (mGluRs), and a down-regulated GABA signaling (Bear et al., 2004), leading to a pronounced excitatory/inhibitory (E:I) imbalance (Contractor et al., 2015). Following this theory, a specific mGluR5 antagonist, the AFQ056/Mavoglurant, has been developed to block the excessive signaling downstream of mGluR5. Interestingly, animal studies showed that AFQ056/Mavoglurant treatment was able to improve maladaptive social behavior (Gantois et al., 2013) and to renormalize plasticity by

* Corresponding author. Neural Control of Movement Lab, Department of Health Sciences and Technology, ETH Zürich, Winterthurerstrasse 190, 8057, Zürich, Switzerland.
E-mail address: valerio.zerbi@hest.ethz.ch (V. Zerbi).

https://doi.org/10.1016/j.neuroimage.2019.02.051
Received 12 July 2018; Received in revised form 11 February 2019; Accepted 19 February 2019
Available online 23 February 2019

correcting abnormal dendritic spine length in *Fmr1*$^{-/y}$ mice (Pop et al., 2014) making it a potential drug that might alleviate key features in FXS.

Driven by the success of preclinical studies, FXS has become the most translated neurodevelopmental disorder in human clinical trials, with the majority of interventional approaches targeting the aforementioned E:I imbalances either with mGluRs antagonist, GABA agonist or both (Duy and Budimirovic, 2017). Yet over the last years, these studies failed to meet their primary efficacy endpoints, including two well-powered, randomized, double-blind, placebo-controlled trials that studied the effect AFQ056/Mavoglurant (Berry-Kravis et al., 2016) or Basimglurant (Youssef et al., 2018) on FXS in humans. These negative results illustrate the gap and challenges of translating therapies from animal models to humans with FXS and ASD. Two fundamental criticisms concern the use of behavioral readouts to determine treatments efficacy in both preclinical and clinical studies: first, despite large efforts for the standardization of behavioral test in animals, the difficulty of identifying robust and reliable behavioral outcome measures suitable for neurobiological studies and drug screenings remains a major limitation. Additionally, there is a general skepticism whether readouts of complex behavior such as sociability are fully translatable from mouse to human (de Esch et al., 2015). Second, assessing clinical efficiency in human patients solely by questionnaires and behavioral scores makes it difficult to differentiate whether a drug treat symptoms or targets specific biological disease pathways. Therefore, there is urgent need for more objective and quantifiable translational biomarkers for monitoring disease progression in response to drug-therapy.

In recent years, MRI-based neuroimaging methods that capture functional and structural connectivity have emerged as tools to evaluate brain functionality in psychiatric disorders. In FXS patients, studies using resting-state functional MRI as a putative marker of E:I imbalance frequently reported alterations of long-range functional connectivity (Hall et al., 2013; van der Molen et al., 2014). White matter microstructural abnormalities were also described in FXS (Villalon-Reina et al., 2013; Wang et al., 2012) and proposed as endogenous neural hallmarks of the syndrome. In our previous work, we demonstrated that *Fmr1*$^{-/y}$ mice display reduced functional connectivity and white-matter anisotropy (Haberl et al., 2015; Zerbi et al., 2018) that are compatible with previous findings of axonal outgrowth and deficits in spine morphology and have strong analogy to observations in humans FXS subjects (Hall et al., 2013, 2016; van der Molen et al., 2014). These studies advocate that neuroimaging might provide sensitive and translational markers of the disease state, which could be integrated in the drug discovery and development pipeline, thereby overcoming the limitations associated with behavioral phenotyping (de Esch et al., 2015) or at least complement these readouts. Yet, to date it is unknown whether MRI connectivity measurements are suited to map changes caused by interventions targeting the receptor level and, particularly, mGluR5 activity since no drug-interventional study has been performed using brain connectivity as primary outcome to score drug efficacy.

Here we show that applying resting state fMRI after inhibiting the activity of the mGluR5 pharmacologically via AFQ056/Mavoglurant in *Fmr1*$^{-/y}$ mice reveals re-normalization of functional connectivity in some but not all of the affected circuits while tests of social interaction display only a trend towards rescuing social behavior.

2. Materials and methods

2.1. Mice

All experiments were performed in accordance with the Swiss federal guidelines for the use of animals in research, and under licensing from the Zürich Cantonal veterinary office. Fmr1 knockout (Fmr1$^{-/y}$) (Mientjes et al., 2006) were bred at the ETH animal facility (*EPIC*, Zürich, Switzerland) and kept on C57Bl/6j background for at least 8 generations. Animals were caged in standard housing, with food and water *ad libitum*, and a 12 h day/night cycle. The experimenter was blind to the genotype for all experiments.

2.2. Drug treatment

At 8 ± 1 weeks of age, Fmr1$^{-/y}$ and their non-transgenic littermates (Fmr1$^{+/y}$) were randomly assigned to two groups receiving either chronic administration of AFQ056/Mavoglurant *via* food pellets (Fmr1$^{-/y}$: n = 14; Fmr1$^{+/y}$: n = 13) or a control standard rodent chow (Fmr1$^{-/y}$: n = 12; Fmr1$^{+/y}$: n = 10). Based on an average intake of 3 g food pellets per day and a body weight of approximately 25 g a dose of 18 mg/kg/day is established. At this dosage, the AFQ056/Mavoglurant passes the blood brain barrier and is effectively delivered to the brain (Gantois et al., 2013). Based on previous pharmacokinetic experiments (Gantois et al., 2013), we expect this mode of administration and dose to induce an almost complete inhibition of the metabotropic glutamate receptor 5. Three weeks after the start of the treatment, mice were evaluated with a three-chambered test to assess sociability and social novelty preference (SPSN). Two weeks later, while still under treatment, mice underwent MRI for the evaluation of structural and functional connectivity.

2.3. Sociability/preference for social novelty (SPSN) task

The SPSN task was a modified version of a protocol described by Nadler and colleagues (Nadler et al., 2004). The setup was made of transparent Plexiglass and consisted of 3 chambers. The central chamber (39 cm × 19 cm × 30 cm) was divided from a left and right chamber of the same size by sliding doors. Left and right chamber contained cylindrical wire cups (10 cm diameter) that could contain stranger mice. Stranger mice used during the test were C57Bl/6j adult, male animals. Testing comprised three assays: acclimation assay, sociability assay (trial 1) and preference for social novelty assay (trial 2). During the acclimation assay, the test mouse was placed in the central compartment for 5 min without access to the left and right chamber. During the sociability assay, a stranger mouse (STR1) was placed into the wire cup randomly in either the left or right chamber. The other chamber contained an empty wire cup. Sliding doors were opened and the test mouse could freely explore all three chambers. After 15 min, the test mouse was guided into the central compartment and sliding doors were closed. A second stranger mouse (STR2) was placed in the remaining wire cup while STR1 stayed in its wire cage. The divider doors were opened for a 15 min exploration of the 3 chambers. Preferential exploration of STR1 over the empty cup (sociability assay) and STR2 over STR1 (preference for social novelty assay) were recorded and analyzed. Explorative social behavior towards stranger mice was scored using Video Tracking System software (Stoelting Co., IL, USA). Time spent in each chamber, number of nose-to-nose contacts and total distance travelled as well as velocity were calculated. Mice were tested in the morning and early afternoon, during the light phase.

2.4. Magnetic resonance imaging

Data acquisition was performed on a Biospec 70/16 small animal MR system (Bruker BioSpin MRI, Ettlingen, Germany) with a cryogenic quadrature surface coil (Bruker BioSpin AG, Fällanden, Switzerland). After standard adjustments, shim gradients were optimized using mapshim protocol, with an ellipsoid reference volume covering the whole brain. For functional connectivity acquisition, a standard gradient-echo echo planar imaging sequence (GE-EPI, repetition time TR = 1000 ms, echo time TE = 15 ms, in-plane resolution RES = 0.22 × 0.2 mm^2, number of slice NS = 20, slice thickness ST = 0.4 mm, slice gap SG = 0.1 mm) was applied to acquire 2000 vol in 38 min. In addition, we acquired anatomical T2*-weighted images (FLASH sequence, in-plane resolution of 0.05 × 0.02 mm, TE = 3.51, TR = 522 ms) and diffusion weighted images (DWI, multi-shot SE-EPI sequence, 4 segments, TR = 2000 ms, TE = 22 ms, RES = 0.2 × 0.2 mm^2, NS = 28, ST = 0.4 mm, SG = 0 mm, 5 b0 images, b-values = 1000-2000 s/mm^2, 90 direction encoding for each

b-value, for a total amount of 185 whole-brain diffusion images and a total scan time of 18 min). The levels of anesthesia and mouse physiological parameters were monitored following an established protocol to obtain a reliable measurement of functional connectivity (Grandjean et al., 2014; Zerbi et al., 2015). Briefly, anesthesia was induced with 4% isoflurane and the animals were endotracheally intubated and the tail vein cannulated. Mice were positioned on a MRI-compatible cradle, and artificially ventilated at 80 breaths per minute, 1:4 O_2 to air ratio, and 1.8 ml/h flow (CWE, Ardmore, USA). A bolus injection of medetomidine 0.05 mg/kg and pancuronium bromide 0.2 mg/kg was administered, and isoflurane was reduced to 1%. After 5 min, an infusion of medetomidine 0.1 mg/kg/h and pancuronium bromide 0.4 mg/kg/h was administered, and isoflurane was further reduced to 0.5%. The animal temperature was monitored using a rectal thermometer probe, and maintained at 36.5 °C ± 0.5 during the measurements. The preparation of the animals did not exceed 20 min.

2.4.1. Resting-state fMRI data pre-processing and analysis

Resting state fMRI datasets were preprocessed using an existing pipeline for removal of unwanted confounds from the time-series using FSL-FIX, adapted for the mouse (Griffanti et al., 2014; Zerbi et al., 2015). After de-spiking (Patel et al., 2014b), we applied an automatic independent component analysis (ICA) classification for the discrimination between true signals versus structured noise components, which includes motion correction and regression; thereafter, data sets were band-pass filtered (0.01–0.3 Hz), skull-stripped and normalized to the AMBMC template (www.imaging.org.au/AMBMC) using ANTs v2.1 (picsl.upenn.edu/ANTS). BOLD time series were extracted using the Allen Reference Atlas ontology (Oh et al., 2014) and their connectivity couplings were measured using regularized Pearson's correlation coefficient (FSLNets), which were Z-scored before statistical analyses. Only macro-areas that were fully covered by the field of view used for rs-fMRI acquisition were included in the analysis (isocortex, hippocampal formation, cortical subplate, striatum, pallidum, thalamus, hypothalamus and midbrain) and consisted of 65 ROIs in each hemisphere. Olfactory bulb and cerebellum were not included in the analysis because of the limited FOV in the axial plane (distance from Bregma: from 2.80 to −6.20) and because of EPI distortion that may occur on these regions, compromising their normalization accuracy.

To probe which specific functional connections showed significant group differences we used the *network-based statistic* method (NBS)(Zalesky et al., 2010) adapted for the mouse functional connectome (Zerbi et al., 2018). Briefly, a general linear model was used to model overall genotype differences, treatment effects, and genotype × treatment interactions. Permutation testing controlled for the family-wise error rate (FWER) by number of graph-network structures in the connectivity matrices using unpaired *t*-tests, with 5000 permutations. A test statistic was then computed for each connection (Z-scored) and a threshold applied ($t = 2.3$) to produce a set of suprathreshold connections, thereby identifying functional networks, which show significant differences in connectivity between groups. In order to remove spurious connections (i.e. those edges that have large variability across individual mice) from the NBS analysis, matrices were given an arbitrary sparsity threshold, retaining only the top-5% of positive connections (Fig. 2A). This threshold is chosen after we found an exponential relationship between the mean functional connectivity strengths and the coefficients of variation for all the datasets (Spearman's RHO = −0.9794, *p*-value<0.000, Supplementary Fig. 1), demonstrating that edges with an averaged Pearson's r (Z-scored) below 0.15–0.16 have large variability across individual mice, and therefore are not reliably represented by the functional connectome.

2.4.2. Brain network topology

We additionally used GRaph thEoreTical Network Analysis toolbox (GRETNA) to perform a comprehensive analysis on the topology of the whole-brain functional connectome. We included in our analysis six metrics commonly used to describe the organization of the human brain networks in the healthy and the disease situation (i.e. clustering coefficient, local and global efficiency, characteristic path length, modularity and assortativity)(Bullmore and Sporns, 2009; Filippi et al., 2013). Among them are: clustering coefficient (i.e. the probability that the neighbors of a given node in a vertex are also connected to each other), local and global efficiency (i.e. the ability of a network to transmit information at the global and local level, respectively), characteristic path length (i.e. the average number of steps along the shortest paths for all possible pairs of network nodes), modularity (i.e. edge densities in given clusters compared to edge densities between clusters) and assortativity (i.e. the tendency of nodes being connected to similar nodes in a network). These metrics were generated based on weighted resting-state connectivity matrices, with prior sparsity thresholding from 5% to 40%. Network topology was compared to random networks (n = 100) based on a time series randomization and correlation matrix randomization as introduced in Zalesky et al. (2012).

2.4.3. Diffusion tensor parameter estimation

Individual realignment of the diffusion images, eddy current correction and tensor estimation were performed using FSL (for further details see (Zerbi et al., 2013)). Thereafter, fractional anisotropy (FA), mean diffusivity (MD), radial diffusivity (RD) and axonal diffusivity (λ1) maps were calculated. The resulting volumes were spatially normalized to the AMBMC template.

2.5. Statistical analysis

A 2-way multivariate analyses of variance (ANOVA) with genotype and drug-treatment as between group factors were conducted to analyze possible differences and interactions between $Fmr1^{-/y}$ and wild-type littermates, and between AFQ056/Mavoglurant and control treatment. P-values were adjusted to control the FWER using Bonferroni correction. For reasons of clarity, *F* values are not reported in the text. Furthermore, only between-group interactions that reached statistical significance are specified in detail. For statistical analysis of graph-based parameter distributions over different sparsity levels, we used a non-parametric test (Kruskal-Wallis test) corrected for multiple comparisons using statistical hypothesis testing (Dunn's test).

3. Results

Here we present the results of 49 male mice ($Fmr1^{-/y}$, n = 26; $Fmr1^{+/y}$, n = 23), which received either Mavoglurant treatment via food pellets (n = 27) or a matched control diet (n = 22). The age of the animals and the length of treatment was matched between groups, and there were no differences in body-weight at the time of MRI experiments (26±2 g). All mice performed the SPSN test. Two mice died during the MRI scans because of a ventilation pump failure. Two mice were further excluded from the MRI analysis due to a fault in the anesthesia delivery system.

3.1. AFQ056/mavoglurant failed to improve sociability and social novelty interest in $Fmr1^{-/y}$ mice

In the three-chamber test, preference for a specific side was measured as the relative amount of time spent in each zone (i.e. cumulative duration) (Fig. 1).

3.1.1. Sociability

As expected, during the sociability test all mice show a preference towards the stranger side as compared to the middle area or the empty side (Fig. 1A, *main area effect: trial 1, p*-value<0.001) irrespective of genotype or treatment. However, the $Fmr1^{-/y}$ mice showed a significantly reduced number of nose-to-nose contacts compared to their $Fmr1^{+/y}$ littermates (Fig. 1C, *p*-value = 0.001), abnormal behavior that tended to be attenuated with Mavoglurant treatment but this effect did not reach

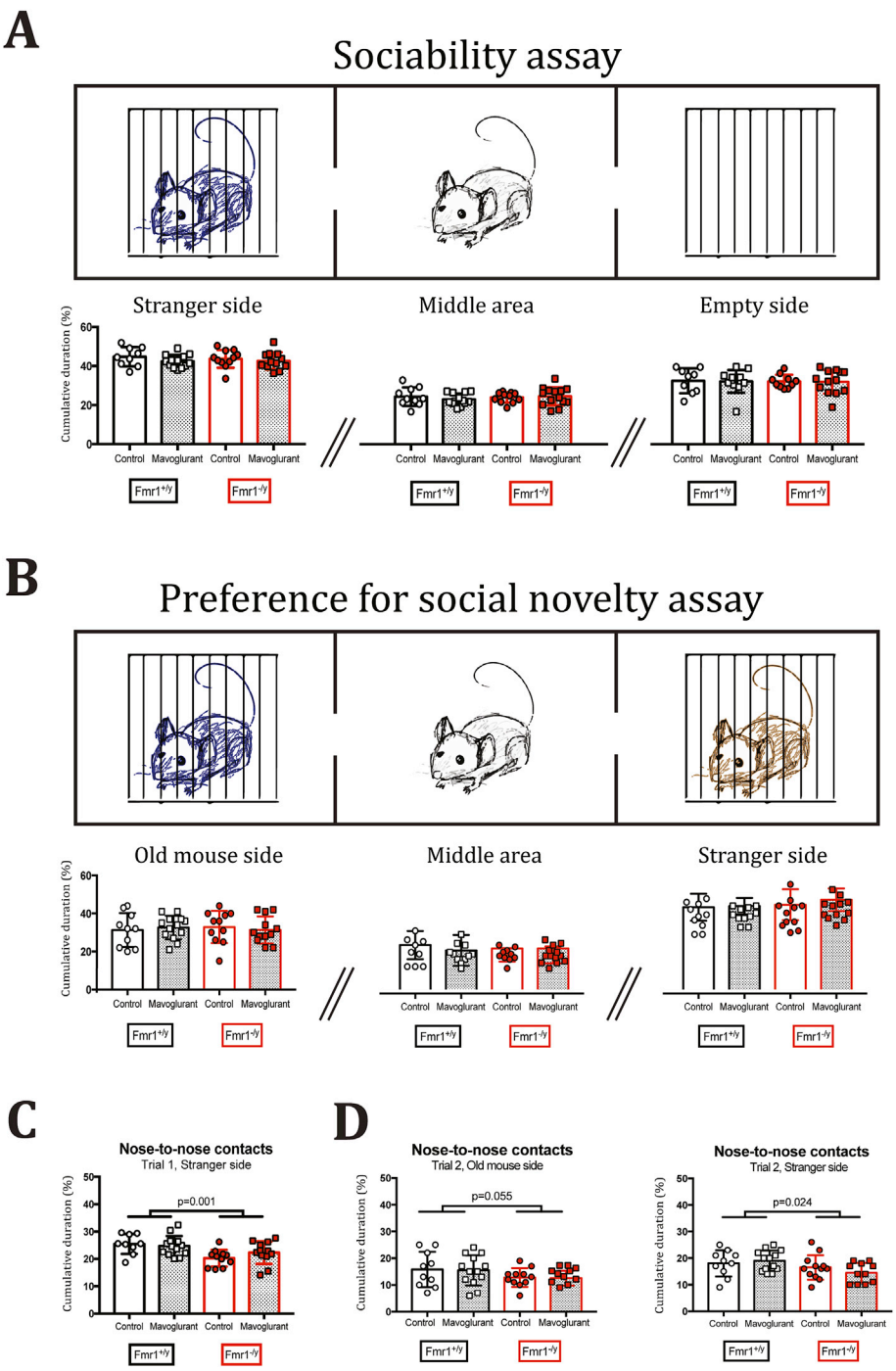

Fig. 1. Sociability and preference for social novelty test revealed reduced social interest in Fmr1KO mice. A) Time spent in the three chambers by untreated and chronic AFQ056/Mavoglurant treated, $Fmr1^{+/y}$ and $Fmr1^{-/y}$ mice. Overall, in the sociability assay all groups spent significantly more time in the stranger side than in the empty and middle areas (p-value<0.001); animals also spent more time in the empty side than in the middle area (p-value = 0.002). However, no effects of genotype, treatment or interactions were found for room preference. B) In the preference for social novelty assay, all mice spent more time in the stranger side than in the old mouse side or middle area (p-value<0.001), suggesting a general increased interest towards the novel social stimulus. C-D) Time spent sniffing (nose-to-nose contacts) during both sociability and social novelty tests revealed an overall genotype effect, with $Fmr1^{+/y}$ mice spent significantly more time than $Fmr1^{-/y}$ in proximity of the stranger mouse (p-value = 0.001 and 0.024, respectively). Chronic treatment with AFQ056/Mavoglurant had little/no effect in restoring this behavior. Error bars show mean ± 95% confidence interval.

statistical significance (genotype × treatment interaction, *p*-value = 0.095).

3.1.2. *Preference for social novelty*

During the social novelty test, all mice spent most of their time on the stranger side and least of their time in the middle area (Fig. 1B, *p*-value<0.001). Similar to the sociability test phase, the $Fmr1^{-/y}$ mice showed significantly reduced interactions with the stranger mouse (Fig. 1D, *p*-value = 0.024) and exhibited a trend towards reduced interactions with the old mouse (*p*-value = 0.055).

Locomotor activity was also measured during the SPSN essay; in both the sociability and social novelty test there were no genotype- or treatment-effects on total distance moved (47.3±7m), mean velocity (5.3 ± 0.9 cm/s) and time spent moving (59 ± 4%) between the groups. However, overall mice were more active during the first sociability trial compared to the preference for social novelty test, indicating a physiological adaptation to the experimental setup (*main trial effect: distance travelled*, *p*-value <0.001; *main trial effect: velocity*, *p*-value <0.001).

3.2. *AFQ056/mavoglurant restored network connectivity in sensory-related areas of $Fmr1^{-/y}$ mice, but not in prefrontal and retrosplenial areas*

Rs-fMRI examines the temporal correlations of slow fluctuations of the blood oxygen level dependent (BOLD) signal across the brain during rest, i.e. without overt perceptual inputs or motor output typically present in traditional fMRI studies. These fluctuations form spatial patterns

of correlated activity that unfold along long-range axonal connections of the brain revealing its intrinsic functional architecture (Zhang and Raichle, 2010).

Permutation testing of 5% sparse BOLD connectomic maps was conducted using Network Based Statistics (NBS)(Zalesky et al., 2010) on both treated and untreated Fmr1$^{+/y}$ and Fmr1$^{-/y}$ mice to evaluate overall group effects and genotype × treatment interactions (Fig. 2). We identified one network with decreased connectivity in Fmr1$^{-/y}$ mice, independent of treatment (Fmr1$^{+/y}$ > Fmr1$^{-/y}$, p-value = 0.032); this network comprises bilateral connections of prefrontal and anterior-posterior cingulate areas (*Anterior-Posterior Cingulate Network*), and extends to the retrosplenial cortex (RSP) and superior colliculus (SC), which are parts of the Default-Mode Network (DMN) in rodents (Sforazzini et al., 2014) (Fig. 2B). Our analysis also revealed that

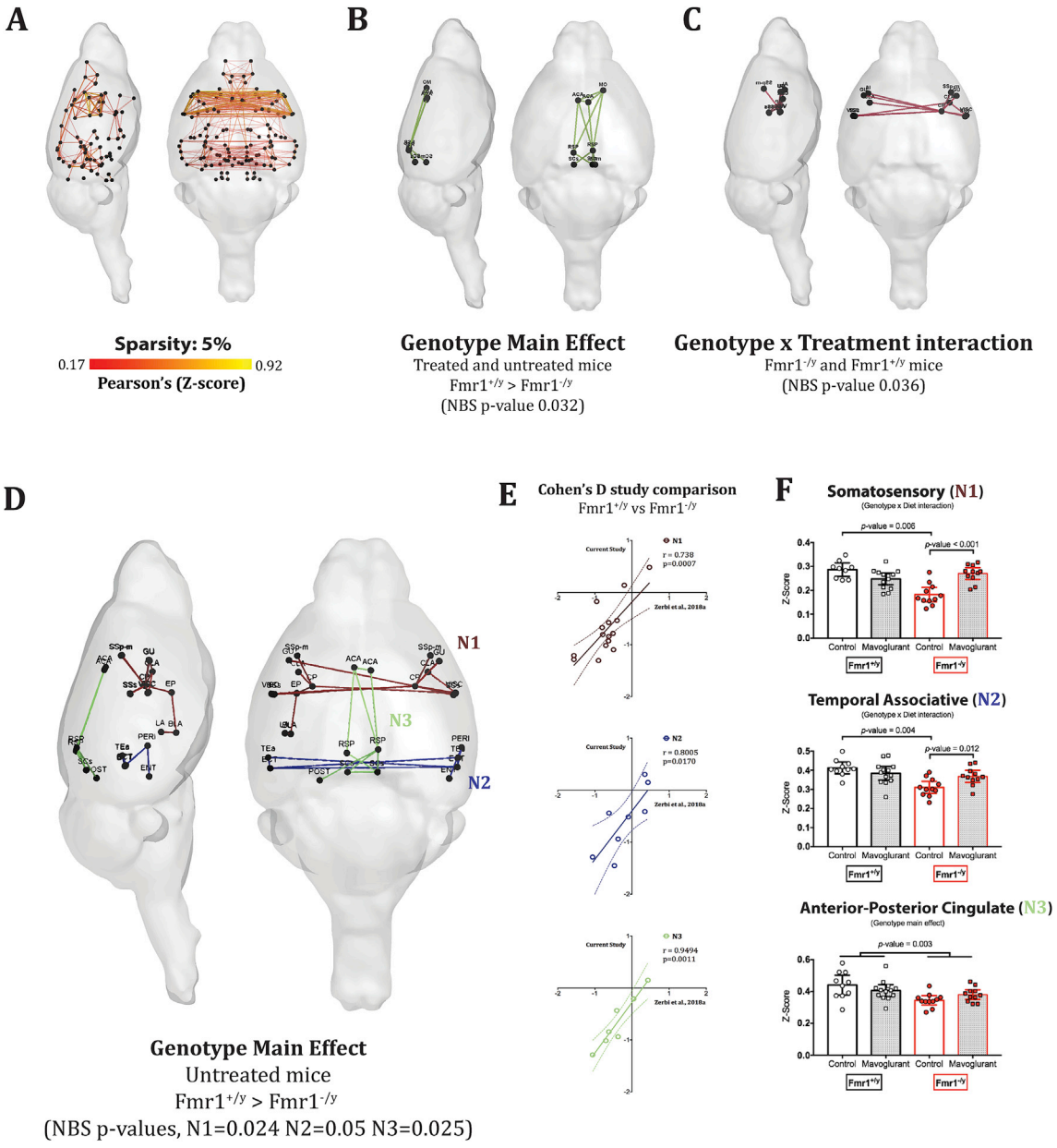

Fig. 2. Resting-state fMRI connectome analysis combined with network based statistics (NBS) detected a hypo-connectivity phenotype in Fmr1$^{-/y}$ mice, which is partly restored by AFQ056/Mavoglurant treatment. A) Graphical representation of the whole-brain functional connectome in the mouse brain, obtained from the average of 46 datasets and thresholded at 5% sparsity. Only these connections are included in the NBS test for group differences. B) Fmr1$^{-/y}$ mice show reduced connectivity between anterior-posterior cingulate, retrosplenial cortex and superior colliculus, independent of treatment (p-value = 0.032). C) Significant genotype × treatment interaction was found between nodes of the somatosensory cortex (bilateral) and striatum. D) Three networks were found hypo-connected in untreated Fmr1$^{-/y}$ mice against untreated Fmr1$^{+/y}$, representing the somatosensory networks (N1, red), the temporal associative (N2, blue) and the anterior-posterior cingulate network (N3, green). E) Scatter plots of effect sizes revealed that connectomic endophenotype of Fmr1$^{-/y}$ mice is reproducible across studies. Cohen's D of individual edges for each hypo-connected network are plotted against the Cohen's D reported in (Zerbi et al., 2018) F) Analyses of network connectivity strength showed that chronic treatment with AFQ056/Mavoglurant was sufficient to restore the connectivity profile towards Fmr1$^{+/y}$ levels in temporal associative and somatosensory networks (Genotype × Treatment interaction, p-value = 0.009 and 0.001, respectively), but not in anterior-posterior cingulate network (p-value = 0.136). Error bars show mean ± 95% confidence interval. Regions affected are as follows: N1) ACA: anterior cingulate area, RSP: retrosplenial cortex, SCs: superior colliculus, sensory related, POST: post-subiculum. N2) SSp-m: primary somatosensory area, mouth; GU: gustatory areas; SSs: supplementary somatosensory area; CLA: claustrum; VISC: visceral cortex; EP: endopiriform nucleus; BLA: basolateral amygdala; LA: lateral amygdala; CP: caudoputamen. N3) TEa: temporal associative area; ECT: ectorhinal cortex; PERI: perirhinal area; ENT: entorhinal area.

somatosensory cortico-striatal areas (*Somatosensory Network*) had both an overall treatment effect (treated > untreated, p-value = 0.001) and a genotype × treatment interaction (p-value = 0.036, Fig. 2C).

For a better evaluation of these interactions, we additionally performed permutation testing in *untreated* Fmr1$^{+/y}$ and Fmr1$^{-/y}$ mice and then confronted the results with ANOVA analyses of network connectivity strength. We identified three networks in which Fmr1$^{-/y}$ mice on control diet had lower connectivity as compared to Fmr1$^{+/y}$ control littermates (Fig. 2D). Specifically, we found a markedly decreased connectivity in: (i) the bilateral *Somatosensory Network*, (p-value = 0.024, N1 in red); (ii) a network that consists of bilateral connections between temporal association area (TEa), entorhinal (ENT) and ectorhinal (ECT) cortex (*Associative Network*, p-value = 0.05, N2 in blue), and in the Anterior-Posterior Cingulate Network (Sforazzini et al., 2014) (p-value = 0.025, N3 in green). In line with earlier reports in Fmr1$^{-/y}$ mice (Haberl et al., 2015; Zerbi et al., 2018) our connectomic approach confirms the robust phenotype displaying reduced FC for specific networks in this mouse model.

In order to quantitatively assess the replicability of connectomic endophenotyping in Fmr1$^{-/y}$ mice, we compared the effect sizes in these three networks (measured as Cohen's D between Fmr1$^{-/y}$ and Fmr1$^{+/y}$ on control diet) with data from our earlier publication (Zerbi et al., 2018) (Supplementary Fig. 2). Specifically, we examined the correlation between Cohen's D in each edge of the identified networks (Somatosensory N1; Temporal Associative N2 and Anterior-Posterior Cingulate N3) (Fig. 2E). We found a strong correlation in the effect sizes for edges of the somatosensory-striatal network (N1, Pearson's correlation test: r = 0.738, P(two-tailed) = 0.0007), the temporal associative network (N2, r = 0.9494, P(two-tailed) = 0.0011), and the anterior-posterior cingulate network (N3, r = 0.8005, P(two-tailed) = 0.0170). In most of the edges and for both studies, the Cohen's D values are negative, highlighting the marked hypo-connectivity phenotype of the Fmr1$^{-/y}$ mouse model.

Importantly, in two of these networks (Somatosensory and Associative) Fmr1$^{-/y}$ treated with Mavoglurant showed significantly higher functional connectivity (towards the levels of Fmr1$^{+/y}$ animals) as compared to the untreated Fmr1$^{-/y}$ mice, suggesting that inhibiting mGluR5 activity rescued long-range connectivity specifically within these circuits (Fig. 2F).

3.3. *Mouse brain functional connectome exhibits non-random, small-world, and efficient network topology. AFQ056/mavoglurant improved local efficiency in Fmr1$^{-/y}$ mice*

We then analyzed whether global network proprieties were also affected in Fmr1$^{-/y}$ mice. Compared to 100 matched random networks with preserved number of nodes/edges and equal connectivity distribution (Zalesky et al., 2012), the mouse functional connectome exhibited efficient small-world proprieties typical of biological systems, such as higher clustering coefficient, path length, modularity, assortativity and local efficiency, as well as lower global efficiency (for all metrics,

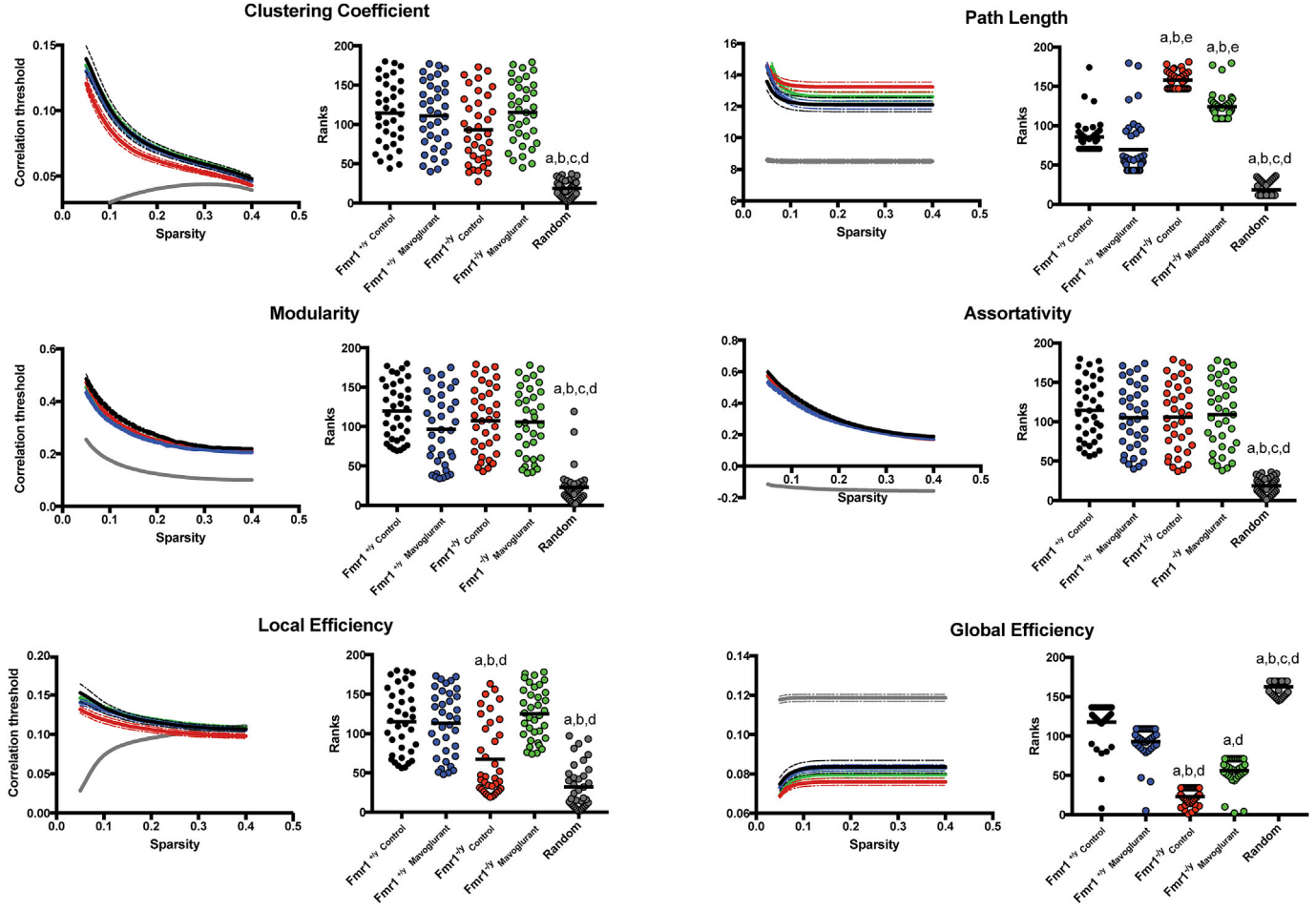

Fig. 3. Graph-theory analysis of mouse brain network characteristics revealed genotype and treatment interactions. Distributions of connectome network proprieties at different sparsity levels were compared between groups and N = 100 random networks. Overall, Fmr1$^{-/y}$ mice show reduced local and global efficiency, with increased path length. Chronic AFQ056/Mavoglurant treatment only marginally improved global efficiency and path length. a: $p < 0.01$ as compared with Fmr1$^{+/y}$ control. b: $p < 0.01$ as compared with Fmr1$^{+/y}$ mavoglurant. c: $p < 0.01$ as compared with Fmr1$^{-/y}$ control. d: $p < 0.01$ as compared with Fmr1$^{-/y}$ mavoglurant. e: $p < 0.01$ as compared with random networks with preserved number of nodes/edges and equal connectivity distribution.

adjusted *p-value*$<10^{-6}$). All these findings were robust against the selection of sparsity levels, suggesting that these organizational principles are stable configurations embedded in the functional brain networks (Fig. 3). Overall, these results are largely comparable with previous functional brain network studies in humans (Bullmore and Sporns, 2009), and connectomic studies in rodents based on tracer data (van den Heuvel et al., 2016), therefore demonstrating the consistency of brain connectome network topology across species and modalities.

Additionally, we noted that untreated $Fmr1^{-/y}$ mice have reduced local (Mean rank difference, MRD = 47.5, adjusted *p*-value = 0.0011) and global efficiency (MRD = 94.7, adjusted *p*-value$<10^{-5}$), and increase in path length compared to $Fmr1^{+/y}$ littermates (MRD = -72.4, adjusted *p*-value$<10^{-5}$). Local efficiency was fully restored by AFQ056/Mavoglurant treatment ($Fmr1^{+/y}$ $_{Mavoglurant}$ vs. $Fmr1^{-/y}$ $_{Mavoglurant}$: MRD = -11.9, adjusted *p*-value>0.999; $Fmr1^{-/y}$ $_{Control}$ vs. $Fmr1^{-/y}$ $_{Mavoglurant}$: MRD = -57.6, adjusted *p*-value$<10^{-5}$), while path length ($Fmr1^{+/y}$ $_{Mavoglurant}$ vs. $Fmr1^{-/y}$ $_{Mavoglurant}$: MRD = -54.4, adjusted *p*-value $<10^{-5}$; $Fmr1^{-/y}$ $_{Control}$ vs. $Fmr1^{-/y}$ $_{Mavoglurant}$: MRD = 33.8, adjusted *p*-value = 0.06) and global efficiency ($Fmr1^{+/y}$ $_{Mavoglurant}$ vs. $Fmr1^{-/y}$ $_{Mavoglurant}$: MRD = 36.8, adjusted *p*-value = 0.027; $Fmr1^{-/y}$ $_{Control}$ vs. $Fmr1^{-/y}$ $_{Mavoglurant}$: MRD = -33.1, adjusted *p*-value = 0.069) showed moderate, but not significant effects of treatment of $Fmr1^{-/y}$ mice (Fig. 3).

3.4. *$Fmr1^{-/y}$ mice show widespread white-matter structural damages, which are not restored by chronic AFQ056/Mavoglurant treatment*

Structural integrity of major axon bundles was quantified by extracting fractional anisotropy (FA) values from eight major white matter structures identified by the Allen Mouse Brain ontology (Zerbi et al., 2018) (Fig. 4). We found marked FA reduction in the $Fmr1^{-/y}$ mice compared to $Fmr1^{+/y}$ littermates in the anterior commissure, corpus callosum, cingulum and cerebral peduncle (*p*-value < 0.01, corrected). Other structures such as the fimbria, ventral hippocampal commissure and internal capsule also showed a moderate decrease in FA (*p*-value < 0.05, corrected). In these same areas, with the exception of internal capsule and cerebral peduncle, we found that the reduced FA was accompanied by a marked increase in radial diffusivity (RD) and a reduction - albeit not significant - in axial diffusivity (λ1) (Fig. 4B). However, we did not detect treatment nor genotype × treatment interactions in any of the white matter structures.

4. Discussion

In this study, we evaluated sociability, whole-brain functional connectivity and white-matter structural abnormalities in mice lacking the FMR1 gene. We used a randomized, controlled design and chronically treated the mice with mGluR5 antagonist AFQ056/Mavoglurant. When compared to non-transgenic littermates, $Fmr1^{-/y}$ mice showed reduced sociability as indicated by less nose-to-nose contacts in a three-chamber test and hypo-connectivity of somatosensory cortico-striatal, temporal association -sensory related- and prefrontal areas (i.e. the mouse equivalent of the Default Mode Network). Network topology also was significantly impaired in $Fmr1^{-/y}$ mice, which showed reduced local and global efficiency, and increased characteristic path length. These functional deficits were accompanied by structural aberrations as indicated by impaired water diffusivity in several white-matter tracts. AFQ056/Mavoglurant treatment restored network connectivity towards the level of non-transgenic mice in sensory-related networks, but not in the anterior-posterior cingulate network. AFQ056/Mavoglurant failed to improve macrostructural white matter deficits and did neither improve sociability nor social novelty interest in $Fmr1^{-/y}$ mice significantly.

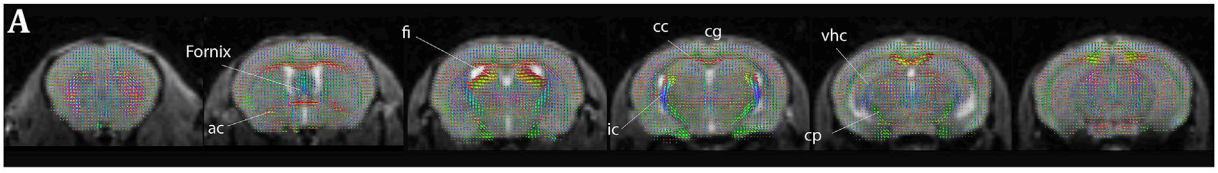

B

	Anterior Commissure	*Fimbria*	*Corpus Callosum*	*Fornix*	*Cingulum*	*Ventral Hippocampal Commissure*	*Internal Capsule*	*Cerebral Peduncle*
Fractional Anisotropy (FA)								
Genotype effects	**.006****	**.028***	**.000****	.466	**.000****	**.014***	**.046***	**.002****
Treatment effects	.574	.447	.242	.723	.486	.743	.519	.991
Interactions	.524	.449	.462	.077	.699	.165	.597	.262
Radial Diffusivity (RD)								
Genotype effects	**.001****	**.013***	**.001****	.502	**.002****	**.000****	.060	.078
Treatment effects	.88	.302	.876	.657	.539	.493	.643	.863
Interactions	.362	.307	.640	.035	.675	.209	.185	.073
Axial Diffusivity (λ1)								
Genotype effects	.445	.721	.417	.735	.187	.958	.908	.595
Treatment effects	.891	.883	.385	.656	.585	.528	.791	.772
Interactions	.963	.799	.310	.718	.314	.611	.868	.356

Fig. 4. Diffusion Tensor Imaging revealed robust white-matter loss of anisotropy in $Fmr1^{y/-}$, independent of treatment. A) Fractional anisotropy (FA) was assessed by diffusion tensor imaging and quantified in eight large white matter structures indicated by different colors. B) 3D plots of voxel-wise diffusion tensor shapes were used for the delineation and selection of white-matter structures (colors indicated direction of eigenvector belonging to largest eigenvalue; red: left-right, green: ventral-dorsal, blue: rostral-caudal). C) $Fmr1^{-/y}$ mice showed significantly reduced anisotropy of diffusion (FA) in seven fiber bundles, including anterior commissure (ac), fimbria (fi), corpus callosum (cc), cingulum (cg), ventral hippocampal commissure (vhc), internal capsule (ic) and cerebral peduncle (cp). Chronic treatment with AFQ056/Mavoglurant did not rescue nor worsen this phenotype.

4.1. Using social behavior to characterize the Fmr1 phenotype and quantify the efficacy of AFQ056/Mavoglurant reveals conflicting results

The three-chamber test is a commonly used behavioral test to study altered social behavior caused by neuropsychiatric disorders including FXS, ASD and schizophrenia (Kaidanovich-Beilin et al., 2011). In line with previous work, we found that all mice spent more time in the chamber with the stranger mouse compared to the chamber with the novel object or the familiar mouse. Additionally, we observed reduced paired-sniffing time in Fmr1$^{-/y}$ mice in both tasks. This index is considered a better measurement for quantification of social interaction compared with time in chamber, which constitutes rather an explorative measurement (Nadler et al., 2004). Reduced social approach in Fmr1$^{-/y}$ mice was not caused by differences in activity and exploratory behavior since there were no significant differences in total entries, switching-rooms frequency, total distance moved and speed between genotypes, but rather suggests abnormal sociability, social motivation and/or affiliation (Kaidanovich-Beilin et al., 2011; Silverman et al., 2010). Our results confirm the altered social phenotype of Fmr1$^{-/y}$ mice, in line with previous observations for this (Hebert et al., 2014; Heitzer et al., 2013; Mineur et al., 2006) and other ASD-related mouse lines (Silverman et al., 2010). Chronic administration of AFQ056/Mavoglurant did not significantly restore sociability nor social novelty towards non-transgenic littermate levels. These results are in contrast with those from an earlier study by Gantois et al., who reported a rescue of Fmr1$^{-/y}$ behavioral phenotype using the same treatment strategy (doses and duration). Notably, they reported an opposite behavioral phenotype in untreated Fmr1$^{-/y}$ mice, i.e. enhanced (rather than diminished) interactions with the stranger mouse in the social preference task, while no significant changes were observed during preference for social novelty assay (Gantois et al., 2013). Furthermore, they reported a reduced sniffing time in treated knockout mice, which also spent less time in a stranger mouse chamber but more time in the empty chamber, suggesting an absence of exploration preference rather than a real rescue of the phenotype. The discrepancy between these and our results adds to the general inconsistencies across studies using the 3-chamber task in models for autism with some reporting increased (Sorensen et al., 2015; Spencer et al., 2005) and other reporting reduced indices of sociability (Mineur et al., 2006). Several aspects of cognition and anxiety phenotypes of Fmr1$^{-/y}$ mice are also highly variable across published reports, some of which in direct opposition to the clinical FXS phenotype, such as a lack of robust cognitive impairments, enhanced pre-pulse inhibition and reduced anxiety in the mouse model (Kazdoba et al., 2014). This underlines the subtle and rather unstable social phenotype of Fmr1$^{-/y}$ mice, and questions the complex and variable interpretations of this behavioral readout. In addition, small changes in the test procedures between different laboratories and their genetic background has led to substantial variability in the reported behavioral phenotypes of *Fmr1*$^{-/y}$ mice, which are generally of small-to-medium effect size and are arguably not objective outcome markers for evaluating the efficacy of a treatment approach (Bakker and Oostra, 2003; Errijgers and Kooy, 2004; Spencer et al., 2011). Instead, combining multiple neuroimaging methods for endophenotype assessment and preclinical drug screening may have several advantages to complement behavioral testing. For example, (i) it allows the study of multiple brain networks in parallel (both functionally and structurally), (ii) can be used to generate specific and testable hypotheses about which circuit and brain areas are involved in drug regulatory interactions; (iii) notably, endophenotyping in Fmr1$^{-/y}$ mice is highly reproducible across studies and (iii) in FXS it seems to have better face validity than behavioral tests.

4.2. Neuroimaging reveals the efficacy of AFQ056/Mavoglurant at the brain system level

Considering that FXS has a high comorbidity with ASD of approximately 30%, it is believed that a treatment effective in FXS might act through a pathway convergent with other risk genes for autism, which has motivated frequent use of Fmr1$^{-/y}$ mice in drug-development research (Auerbach et al., 2011; Hagerman et al., 2010). Modulating metabotropic glutamate receptor-5 activity has been considered for long time one of the most promising strategies to treat the underlying disorder instead of the symptoms of FXS (Bear et al., 2004). It refers to the *mGluR theory* of FXS, which proposes that inhibition of group mGluR5 signaling might be sufficient to correct the brains' pathophysiology and related behavioral symptomatology. This theory found evidence in preclinical studies, which showed that blocking the excessive signaling downstream of mGluR5 with AFQ056/Mavoglurant treatment is able to reverse structural spine abnormalities observed in Fmr1$^{-/y}$ mice (Pop et al., 2014). However, there was no concrete indication that AFQ056/Mavoglurant could restore the delicate E:I balances at the system level.

The present study fills this gap of knowledge and demonstrates the efficacy of AFQ056/Mavoglurant to re-establish brain connectivity within specific networks and certain aspects of network topology, such that brain's functional connectivity signature of Fmr1$^{-/y}$ mice become more similar to those in wild type controls. Our study also revealed that efficacy of AFQ056/Mavoglurant differs across brain circuits. While it was able to stabilize the functional coupling between nodes of sensory-cortical areas and striatum as well as between the cortical association areas, it did not restore connectivity strength in prefrontal regions and in brain areas constituting the rodent equivalent of the *Default-Mode Network* (DMN).

Specifically, we found that the absence of FMRP translates into hypo-connectivity in brain networks and pathways associated with sensorial processing and perception (i.e. somatosensory-striatal and association cortical connections) and also in the prefrontal-retrosplenial areas. These results replicate and extend previous findings of connectivity deficits in Fmr1$^{-/y}$ mice (Haberl et al., 2015; Zerbi et al., 2018). Furthermore, quantitative comparison of effect sizes in the affected networks demonstrates high reproducibility of the connectivity phenotyping in Fmr1$^{-/y}$ mice and indicates that rs-fMRI is a robust tool for identifying the topography and extent of aberrant brain function linked to FXS pathology. In humans, deficits in associated circuits have been found in both FXS and ASD subjects, and linked to common symptoms such as sensory hypersensitivity, and deficits in attention and sociability (Baron-Cohen et al., 2009; Gallagher and Hallahan, 2012) (Hall et al., 2013; Reig and Silberberg, 2016; Wilson, 2014). Although evidence of a direct link between specific behavioral traits and network coupling in mice are lacking, it is interesting to note that in Fmr1 over-reactivity to somatosensory stimuli are accompanied by a reduced resting-state connectivity of sensory-related regions (He et al., 2017; Rotschafer and Razak, 2013; Zhang et al., 2014). This evidence supports the hypothesis that atypical sensory experience leading to overreactivity may be linked to deficits in neuronal adaptation to sensory stimuli in the cortex (He et al., 2017). While it remains unclear whether AFQ056/Mavoglurant treatment results in an amelioration of sensory-related information processing, our finding suggests that restoration of connectivity in sensory-related networks by AFQ056/Mavoglurant might be a way to treat one common class of abnormal behaviors in FXS and ASD, which relates to hypersensitivity to sensory stimulation. Since hypersensitivity to sensory stimuli is one of the most prominent features of FXS and ASD patients (Baron-Cohen et al., 2009; Gallagher and Hallahan, 2012), future studies are encouraged to clarify the effects of mGluR5 antagonist on these specific behavioral traits.

The application of graph analysis to our functional connectomic data permitted to study the aggregated functional topology of the brain in a few parameters with clear theoretical meaning (Sanz-Arigita et al., 2010), and provided a high-level description of the changes in the global functional state of Fmr1$^{-/y}$ mice. Our results showed that absence of FRMP leads to a reduction of the network's local efficiency and global efficiency and to an increase in characteristic path length. According to principles of the small-world theoretical model, the reduction of local efficiency reveals a deficiency of information transfer between

neighboring nodes in a network, while the increased path length and reduced global efficiency may reflect impairments in the randomization of the functional topology, which is typical of the aged and/or diseased brain (Ajilore et al., 2014). Reduction of network efficiency and information transfer could also be the result of disrupted high degree-centrality nodes (i.e., brain areas with high density of functional connections or "brain hubs" (Fulcher and Fornito, 2016; Liska et al., 2015)), which are key contributors to the optimal small-world network configuration. Thus, loss of efficient inter-cluster connections in $Fmr1^{-/y}$ mice convey the risk of blocking or slowing down the flow of information through the entire brain, which may relate to their behavioral phenotype. MGluR5 inhibition was effective in restoring the local efficiency of $Fmr1^{-/y}$ mice to the $Fmr1^{+/y}$ levels, but only partly restored global efficiency and path length. Overall, this indicate that our treatment was effective in spatially-confined networks (i.e. the somatosensory network), but failed to improve the global network characteristics that heavily depend on brain hubs functionality.

We did not observe rescue of the ultrastructure of major white matter tracts, which represent the anatomical substrate underlying long range functional connectivity (Grandjean et al., 2017). Our diffusion data show that water in white matter bundles diffuses significantly more perpendicularly and less parallelly to the main fiber orientation. This phenomenon explains the reduced fractional anisotropy (FA) observed in the $Fmr1^{-/y}$ model and in FXS patients (Filley, Brown, Onderko, et al., 2015; Hashimoto, Srivastava, Tassone, et al., 2011). As we previously reported a reduction in axonal diameter and G-ratio in $Fmr1^{-/y}$ mice using electron microscopy (Zerbi et al., 2018), this data suggests that the relative increase in extracellular space rather than the reduced intra-axonal space accounts for the increase in radial diffusivity. It is interesting to note that functional hypo-connectivity and structural deficits, which are specific to $Fmr1^{-/y}$ mice manifest during early post-natal development and are maintained throughout adulthood. In line with the pivotal role of FMRP in early embryotic neurodevelopment (Hinds et al., 1993), one could speculate that the sensitive period, which determines the long-range connectivity phenotype of $Fmr1^{-/y}$ mice, may be immediately after or already prior to birth and relates to glial synaptic pruning functioning and myelin development (Patel et al., 2014a). Our results suggest that future studies should investigate the effects of an early intervention of AFQ056/Mavoglurant as a treatment for FXS. Finally, follow-up studies could look at different doses to confirm that the observed change is treatment dependent rather than variation in the technique used.

4.3. Limitations

There are some limitations of this study that must be acknowledged. Whilst rs-fMRI can provide an interesting overview of the functionally architecture at the brain system level, it is nevertheless a proxy measure of neuronal activity and synchronization, and it is tightly linked to the function of the neurovascular unit. Therefore, it would be critical to understand if our findings reflect neural or rather hemodynamic differences between groups. Although we did not measure cerebral blood flow nor peripheral blood pressure during the MRI sessions, there are several arguments making it unlikely that hemodynamic changes could have driven our main results. First, an earlier study extensively demonstrated that mGluR5 inhibition with a prototypic mGluR5 antagonist (MPEP) does not affect cerebral hemodynamic responses in rats (Calcinaghi et al., 2011). Second, the genotype, treatment and treatment × genotype interactions that we report are circuit-specific. A higher or lower sensitivity to the anesthesia in one group would have likely resulted in systemic effects, i.e. an increased or reduced connectivity in various networks, and not just in a few. Finally, we showed in an additional cohort of wildtype animals that cardiovascular parameters stay within the physiological range during the scan session if the animal is being anesthetized with medetomidine/isoflurane and artificially ventilated following the exact same experimental procedure as in the cohorts reported above (Supplementary Table 1).

We found that functional connectivity of the somatosensory and temporal association areas improved after mGluR5 targeting treatment but we were unable to correlate these findings with changes in the behavioral outcome. It should be noted that our behavioral tasks were designed to assess sociability rather than sensory-specific responses. However, recent literature provides first evidence linking Fmr1 expression to hypersensitivity: Chelini and colleagues demonstrated that engrailed-2 knockout mice, which show a lower expression of Fmr1 and anatomical defects common to Fmr1 knockouts, have similar patterns of reduced connectivity in somatosensory, auditory and association cortices, which are associated with increased sensitivity to somatosensory stimuli (Chelini et al., 2018). Moreover, Westmar and colleagues showed that Mavoglurant attenuated audiogenic-induced seizures in $Fmr1^{-/y}$ mice (Westmark et al., 2018). Together, these studies support our hypothesis that impaired somatosensory processing is a common multi-level (i.e. cellular, network, behavioral) feature in mice lacking Fmr1, which might be attenuated by Mavoglurant treatment. Future studies in this direction are warranted to establish a mechanistic link between connectional observations and abnormal behavior in $Fmr1^{-/y}$ mice. Follow-up research could be performed combining neuroimaging with invasive neurostimulaton methods such as reversible cooling deactivation, targeted microstimulation, optogenetics and chemogenetics. These approaches can provide detailed demonstrations of brain-behavior relationships with a high degree of spatial precision, encompassing even cell-type-specific effects.

In our work, we focused primarily on rs-fMRI as a metric to derive functional "connectivity". We have previously demonstrated that the functional connectome is very well in line with the anatomical ground truth provided by viral tracer injections in the mouse brain (i.e. structural connectome) (Grandjean et al., 2017; Sethi et al., 2017). Indeed, **structural** connectivity could also have been obtained non-invasively with tractography by post-processing of diffusion MRI data. However, there are a number of limitations that discouraged us from computing this index. For example, the small size of white matter bundles and the subtle GM/WM interface in the mouse makes it difficult to follow tracks from initiation to termination. Moreover, a recent study found only a moderate similarity between neuronal tracer data and tractography-based connectivity in rats because the latter resulted in a substantial number of false positive and false negative connections (Sinke et al., 2018). This issue was apparent even when using sophisticated tractography algorithms, including multi-shell multi-tissue constrained spherical deconvolution and global tractography. As we tried to replicate their findings with our *in-vivo* data, we noted that the similarity between our DWI-structural connectome and the Allen tracer data for inter-hemispheric cortico-cortico connections was above chance level (Supplementary Fig. 3) but much lower than what observed with rs-fMRI data (Grandjean et al., 2017). For these reasons, we decided not to include structural connectivity comparisons between our models, but we kept the DTI parameters as surrogate measures of white matter structural integrity.

5. Conclusion

Based on preclinical results in $Fmr1^{-/y}$ mice, the modulation of mGluR5 activity via negative allosteric modulators such as AFQ056/Mavoglurant or Basmiglurant held promise as effective treatment for Fragile X mental retardation syndrome. Yet, these results failed to translate into a reversal of behavioral symptoms in FXS patients, illustrating the gaps and challenges of translating therapies from animal models to humans with FXS and ASD (Berry-Kravis et al., 2016; Youssef et al., 2018). Our research introduces a paradigm shift in drug development by complementing behavioral assays in rodents, which suffer from limited translational validity, with imaging biomarkers, in particular resting-state fMRI and diffusion MRI probing functional and structural connectivity. Although it is still unclear how these macroscopic measurements reflect E/I alterations and white matter structural integrity,

both endogenous hallmarks offer unbiased and robust evaluation of brain function and structure at the systems level. Specifically for complex disorders such as FXS, the assessment of these brain-wide, macroscopic measurements might be encouraged in the early phases of preclinical drug-development studies, as it could guide subsequent electrophysiological, histological or further behavioral assessments by providing evidence-based anatomical and circuital hypotheses rather than investigating treatment effects in a process of trial-and-error using reductionistic models. We argue that this is a better strategy for future preclinical drug-screening assessments in psychiatry.

Data from our experiment show that rs-fMRI connectivity is sufficiently sensitive to pick up changes elicited by therapeutic interventions such as the pharmacological inhibition of mGluR5 activity. However, our results also show that the effects of AFQ056/Mavoglurant relate to specific functional networks suggesting that behavioral benefits might be restricted to narrow functional domains, specifically sensory processing and integration. Therefore, we propose that those domains should be re-examined with appropriate tests in the phase II trials of AFQ056/Mavoglurant or Basmiglurant.

Disclosures

All the authors have no conflict of interest to declare.

Acknowledgements

V.Z. is supported by ETH Career Seed Grant SEED-42 16-1 and by the SNSF AMBIZIONE PZ00P3_173984/1. M.M. is supported by ETH Research Grant ETH-38 16-2. F. G. is an employee of Novartis Pharma AG. We thank Dr. Daniel Woolley for proofreading the article.

Appendix A. Supplementary data

Supplementary data to this article can be found online at https://doi.org/10.1016/j.neuroimage.2019.02.051. Preprocessed resting-state fMRI data are available at DOI: 10.3929/ethz-b-000327762. All raw data are available upon request.

References

Ajilore, O., Lamar, M., Kumar, A., 2014. Association of brain network efficiency with aging, depression, and cognition. Am. J. Geriatr. Psychiatry 22, 102–110.
Auerbach, B.D., Osterweil, E.K., Bear, M.F., 2011. Mutations causing syndromic autism define an axis of synaptic pathophysiology. Nature 480, 63–68.
Bakker, C.E., Oostra, B.A., 2003. Understanding fragile X syndrome: insights from animal models. Cytogenet. Genome Res. 100, 111–123.
Baron-Cohen, S., Ashwin, E., Ashwin, C., Tavassoli, T., Chakrabarti, B., 2009. Talent in autism: hyper-systemizing, hyper-attention to detail and sensory hypersensitivity. Philos. Trans. R. Soc. Lond. B Biol. Sci. 364, 1377–1383.
Bear, M.F., Huber, K.M., Warren, S.T., 2004. The mGluR theory of fragile X mental retardation. Trends Neurosci. 27, 370–377.
Berry-Kravis, E., Des Portes, V., Hagerman, R., Jacquemont, S., Charles, P., Visootsak, J., Brinkman, M., Rerat, K., Koumaras, B., Zhu, L., Barth, G.M., Jaecklin, T., Apostol, G., von Raison, F., 2016. Mavoglurant in fragile X syndrome: results of two randomized, double-blind, placebo-controlled trials. Sci. Transl. Med. 8, 321ra325.
Bullmore, E., Sporns, O., 2009. Complex brain networks: graph theoretical analysis of structural and functional systems. Nat. Rev. Neurosci. 10, 186–198.
Calcinaghi, N., Jolivet, R., Wyss, M.T., Ametamey, S.M., Gasparini, F., Buck, A., Weber, B., 2011. Metabotropic glutamate receptor mGluR5 is not involved in the early hemodynamic response. J. Cerebr. Blood Flow Metabol. 31, e1–10.
Chelini, G., Zerbi, V., Cimino, L., Grigoli, A., Markicevic, M., Libera, F., Robbiati, S., Gadler, M., Bronzoni, S., Miorelli, S., Galbusera, A., Gozzi, A., Casarosa, S., Provenzano, G., Bozzi, Y., 2018. Aberrant somatosensory processing and connectivity in mice lacking Engrailed-2. J. Neurosci. 39 (8), 1525–1538.
Contractor, A., Klyachko, V.A., Portera-Cailliau, C., 2015. Altered neuronal and circuit excitability in fragile X syndrome. Neuron 87, 699–715.
de Esch, C.E., van den Berg, W.E., Buijsen, R.A., Jaafar, I.A., Nieuwenhuizen-Bakker, I.M., Gasparini, F., Kushner, S.A., Willemsen, R., 2015. Fragile X mice have robust mGluR5-dependent alterations of social behaviour in the Automated Tube Test. Neurobiol. Dis. 75, 31–39.
Duy, P.Q., Budimirovic, D.B., 2017. Fragile X syndrome: lessons learned from the most translated neurodevelopmental disorder in clinical trials. Transl. Neurosci. 8, 7–8.
Dyer-Friedman, J., Glaser, B., Hessl, D., Johnston, C., Huffman, L.C., Taylor, A., Wisbeck, J., Reiss, A.L., 2002. Genetic and environmental influences on the cognitive outcomes of children with fragile X syndrome. J. Am. Acad. Child Adolesc. Psychiatry 41, 237–244.
Errijgers, V., Kooy, R.F., 2004. Genetic modifiers in mice: the example of the fragile X mouse model. Cytogenet. Genome Res. 105, 448–454.
Filippi, M., van den Heuvel, M.P., Fornito, A., He, Y., Hulshoff Pol, H.E., Agosta, F., Comi, G., Rocca, M.A., 2013. Assessment of system dysfunction in the brain through MRI-based connectomics. Lancet Neurol. 12, 1189–1199.
Filley, C.M., Brown, M.S., Onderko, K., Ray, M., Bennett, R.E., Berry-Kravis, E., Grigsby, J., 2015. White matter disease and cognitive impairment in FMR1 premutation carriers. Neurology. 84 (21), 2146–2152.
Fulcher, B.D., Fornito, A., 2016. A transcriptional signature of hub connectivity in the mouse connectome. Proc. Natl. Acad. Sci. U. S. A 113, 1435–1440.
Gallagher, A., Hallahan, B., 2012. Fragile X-associated disorders: a clinical overview. J. Neurol. 259, 401–413.
Gantois, I., Pop, A.S., de Esch, C.E., Buijsen, R.A., Pooters, T., Gomez-Mancilla, B., Gasparini, F., Oostra, B.A., D'Hooge, R., Willemsen, R., 2013. Chronic administration of AFQ056/Mavoglurant restores social behaviour in Fmr1 knockout mice. Behav. Brain Res. 239, 72–79.
Glass, I.A., 1991. X linked mental retardation. J. Med. Genet. 28, 361–371.
Grandjean, J., Schroeter, A., Batata, I., Rudin, M., 2014. Optimization of anesthesia protocol for resting-state fMRI in mice based on differential effects of anesthetics on functional connectivity patterns. Neuroimage 102 Pt 2, 838–847.
Grandjean, J., Zerbi, V., Balsters, J.H., Wenderoth, N., Rudin, M., 2017. Structural basis of large-scale functional connectivity in the mouse. J. Neurosci. 37, 8092–8101.
Griffanti, L., Salimi-Khorshidi, G., Beckmann, C.F., Auerbach, E.J., Douaud, G., Sexton, C.E., Zsoldos, E., Ebmeier, K.P., Filippini, N., Mackay, C.E., Moeller, S., Xu, J., Yacoub, E., Baselli, G., Ugurbil, K., Miller, K.L., Smith, S.M., 2014. ICA-based artefact removal and accelerated fMRI acquisition for improved resting state network imaging. Neuroimage 95, 232–247.
Haberl, M.G., Zerbi, V., Veltien, A., Ginger, M., Heerschap, A., Frick, A., 2015. Structural-functional connectivity deficits of neocortical circuits in the Fmr1 (-/y) mouse model of autism. Sci Adv 1 e1500775.
Hagerman, R., Hoem, G., Hagerman, P., 2010. Fragile X and autism: intertwined at the molecular level leading to targeted treatments. Mol. Autism. 1, 12.
Hall, S.S., Dougherty, R.F., Reiss, A.L., 2016. Profiles of aberrant white matter microstructure in fragile X syndrome. Neuroimage Clin 11, 133–138.
Hall, S.S., Jiang, H., Reiss, A.L., Greicius, M.D., 2013. Identifying large-scale brain networks in fragile x syndrome. JAMA Psychiatry 70, 1215–1223.
Hashimoto, R., Srivastava, S., Tassone, F., Hagerman, R.J., Rivera, S.M., 2011. Diffusion tensor imaging in male premutation carriers of the fragile X mental retardation gene. Mov Disord 26 (7), 1329–1336.
He, C.X., Cantu, D.A., Mantri, S.S., Zeiger, W.A., Goel, A., Portera-Cailliau, C., 2017. Tactile defensiveness and impaired adaptation of neuronal activity in the Fmr1 knock-out mouse model of autism. J. Neurosci. 37, 6475–6487.
Hebert, B., Pietropaolo, S., Meme, S., Laudier, B., Laugeray, A., Doisne, N., Quartier, A., Lefeuvre, S., Got, L., Cahard, D., Laumonnier, F., Crusio, W.E., Pichon, J., Menuet, A., Perche, O., Briault, S., 2014. Rescue of fragile X syndrome phenotypes in Fmr1 KO mice by a BKCa channel opener molecule. Orphanet J. Rare Dis. 9, 124.
Heitzer, A.M., Roth, A.K., Nawrocki, L., Wrenn, C.C., Valdovinos, M.G., 2013. Brief report: altered social behavior in isolation-reared Fmr1 knockout mice. J. Autism Dev. Disord. 43, 1452–1458.
Hinds, H.L., Ashley, C.T., Sutcliffe, J.S., Nelson, D.L., Warren, S.T., Housman, D.E., Schalling, M., 1993. Tissue specific expression of FMR-1 provides evidence for a functional role in fragile X syndrome. Nat. Genet. 3, 36–43.
Kaidanovich-Beilin, O., Lipina, T., Vukobradovic, I., Roder, J., Woodgett, J.R., 2011. Assessment of social interaction behaviors. JoVE in press.
Kazdoba, T.M., Leach, P.T., Silverman, J.L., Crawley, J.N., 2014. Modeling fragile X syndrome in the Fmr1 knockout mouse. Intractable Rare Dis Res 3, 118–133.
Liska, A., Galbusera, A., Schwarz, A.J., Gozzi, A., 2015. Functional connectivity hubs of the mouse brain. Neuroimage 115, 281–291.
Loesch, D.Z., Huggins, R.M., Hagerman, R.J., 2004. Phenotypic variation and FMRP levels in fragile X. Ment. Retard. Dev. Disabil. Res. Rev. 10, 31–41.
Mientjes, E.J., Nieuwenhuizen, I., Kirkpatrick, L., Zu, T., Hoogeveen-Westerveld, M., Severijnen, L., Rife, M., Willemsen, R., Nelson, D.L., Oostra, B.A., 2006. The generation of a conditional Fmr1 knock out mouse model to study Fmrp function in vivo. Neurobiol. Dis. 21, 549–555.
Mineur, Y.S., Huynh, L.X., Crusio, W.E., 2006. Social behavior deficits in the Fmr1 mutant mouse. Behav. Brain Res. 168, 172–175.
Nadler, J.J., Moy, S.S., Dold, G., Trang, D., Simmons, N., Perez, A., Young, N.B., Barbaro, R.P., Piven, J., Magnuson, T.R., Crawley, J.N., 2004. Automated apparatus for quantitation of social approach behaviors in mice. Genes Brain Behav. 3, 303–314.
Oh, S.W., Harris, J.A., Ng, L., Winslow, B., Cain, N., Mihalas, S., Wang, Q., Lau, C., Kuan, L., Henry, A.M., Mortrud, M.T., Ouellette, B., Nguyen, T.N., Sorensen, S.A., Slaughterbeck, C.R., Wakeman, W., Li, Y., Feng, D., Ho, A., Nicholas, E., Hirokawa, K.E., Bohn, P., Joines, K.M., Peng, H., Hawrylycz, M.J., Phillips, J.W., Hohmann, J.G., Wohnoutka, P., Gerfen, C.R., Koch, C., Bernard, A., Dang, C., Jones, A.R., Zeng, H., 2014. A mesoscale connectome of the mouse brain. Nature 508, 207–214.
Patel, A.B., Loerwald, K.W., Huber, K.M., Gibson, J.R., 2014a. Postsynaptic FMRP promotes the pruning of cell-to-cell connections among pyramidal neurons in the L5A neocortical network. J. Neurosci. 34, 3413–3418.
Patel, A.X., Kundu, P., Rubinov, M., Jones, P.S., Vertes, P.E., Ersche, K.D., Suckling, J., Bullmore, E.T., 2014b. A wavelet method for modeling and despiking motion artifacts from resting-state fMRI time series. Neuroimage 95, 287–304.

Pieretti, M., Zhang, F.P., Fu, Y.H., Warren, S.T., Oostra, B.A., Caskey, C.T., Nelson, D.L., 1991. Absence of expression of the FMR-1 gene in fragile X syndrome. Cell 66, 817–822.
Pop, A.S., Levenga, J., de Esch, C.E., Buijsen, R.A., Nieuwenhuizen, I.M., Li, T., Isaacs, A., Gasparini, F., Oostra, B.A., Willemsen, R., 2014. Rescue of dendritic spine phenotype in Fmr1 KO mice with the mGluR5 antagonist AFQ056/Mavoglurant. Psychopharmacology (Berlin) 231, 1227–1235.
Reig, R., Silberberg, G., 2016. Distinct corticostriatal and intracortical pathways mediate bilateral sensory responses in the striatum. Cerebr. Cortex 26, 4405–4415.
Rotschafer, S., Razak, K., 2013. Altered auditory processing in a mouse model of fragile X syndrome. Brain Res. 1506, 12–24.
Sanz-Arigita, E.J., Schoonheim, M.M., Damoiseaux, J.S., Rombouts, S.A., Maris, E., Barkhof, F., Scheltens, P., Stam, C.J., 2010. Loss of 'small-world' networks in Alzheimer's disease: graph analysis of FMRI resting-state functional connectivity. PLoS One 5 e13788.
Sethi, S.S., Zerbi, V., Wenderoth, N., Fornito, A., Fulcher, B.D., 2017. Structural connectome topology relates to regional BOLD signal dynamics in the mouse brain. Chaos 27, 047405.
Sforazzini, F., Schwarz, A.J., Galbusera, A., Bifone, A., Gozzi, A., 2014. Distributed BOLD and CBV-weighted resting-state networks in the mouse brain. Neuroimage 87, 403–415.
Silverman, J.L., Yang, M., Lord, C., Crawley, J.N., 2010. Behavioural phenotyping assays for mouse models of autism. Nat. Rev. Neurosci. 11, 490–502.
Sinke, M.R.T., Otte, W.M., Christiaens, D., Schmitt, O., Leemans, A., van der Toorn, A., Sarabdjitsingh, R.A., Joels, M., Dijkhuizen, R.M., 2018. Diffusion MRI-based cortical connectome reconstruction: dependency on tractography procedures and neuroanatomical characteristics. Brain Struct. Funct. 223, 2269–2285.
Sorensen, E.M., Bertelsen, F., Weikop, P., Skovborg, M.M., Banke, T., Drasbek, K.R., Scheel-Kruger, J., 2015. Hyperactivity and lack of social discrimination in the adolescent Fmr1 knockout mouse. Behav. Pharmacol. 26, 733–740.
Spencer, C.M., Alekseyenko, O., Hamilton, S.M., Thomas, A.M., Serysheva, E., Yuva-Paylor, L.A., Paylor, R., 2011. Modifying behavioral phenotypes in Fmr1KO mice: genetic background differences reveal autistic-like responses. Autism Res. 4, 40–56.
Spencer, C.M., Alekseyenko, O., Serysheva, E., Yuva-Paylor, L.A., Paylor, R., 2005. Altered anxiety-related and social behaviors in the Fmr1 knockout mouse model of fragile X syndrome. Genes Brain Behav. 4, 420–430.
Tassone, F., Hagerman, R.J., Ikle, D.N., Dyer, P.N., Lampe, M., Willemsen, R., Oostra, B.A., Taylor, A.K., 1999. FMRP expression as a potential prognostic indicator in fragile X syndrome. Am. J. Med. Genet. 84, 250–261.
van den Heuvel, M.P., Scholtens, L.H., de Reus, M.A., 2016. Topological organization of connectivity strength in the rat connectome. Brain Struct. Funct. 221, 1719–1736.
van der Molen, M.J., Stam, C.J., van der Molen, M.W., 2014. Resting-state EEG oscillatory dynamics in fragile X syndrome: abnormal functional connectivity and brain network organization. PLoS One 9, e88451.
Villalon-Reina, J., Jahanshad, N., Beaton, E., Toga, A.W., Thompson, P.M., Simon, T.J., 2013. White matter microstructural abnormalities in girls with chromosome 22q11.2 deletion syndrome, Fragile X or Turner syndrome as evidenced by diffusion tensor imaging. Neuroimage 81, 441–454.
Wang, J.Y., Hessl, D.H., Hagerman, R.J., Tassone, F., Rivera, S.M., 2012. Age-dependent structural connectivity effects in fragile x premutation. Arch. Neurol. 69, 482–489.
Westmark, P.R., Dekundy, A., Gravius, A., Danysz, W., Westmark, C.J., 2018. Rescue of Fmr1(KO) phenotypes with mGluR5 inhibitors: MRZ-8456 versus AFQ-056. Neurobiol. Dis. 119, 190–198.
Willemsen, R., Levenga, J., Oostra, B.A., 2011. CGG repeat in the FMR1 gene: size matters. Clin. Genet. 80, 214–225.
Wilson, C.J., 2014. The sensory striatum. Neuron 83, 999–1001.
Youssef, E.A., Berry-Kravis, E., Czech, C., Hagerman, R.J., Hessl, D., Wong, C.Y., Rabbia, M., Deptula, D., John, A., Kinch, R., Drewitt, P., Lindemann, L., Marcinowski, M., Langland, R., Horn, C., Fontoura, P., Santarelli, L., Quiroz, J.A., FragXis Study, G., 2018. Effect of the mGluR5-NAM basimglurant on behavior in adolescents and adults with fragile X syndrome in a randomized, double-blind, placebo-controlled trial: FragXis phase 2 results. Neuropsychopharmacology 43, 503–512.
Zalesky, A., Fornito, A., Bullmore, E., 2012. On the use of correlation as a measure of network connectivity. Neuroimage 60, 2096–2106.
Zalesky, A., Fornito, A., Bullmore, E.T., 2010. Network-based statistic: identifying differences in brain networks. Neuroimage 53, 1197–1207.
Zerbi, V., Grandjean, J., Rudin, M., Wenderoth, N., 2015. Mapping the mouse brain with rs-fMRI: an optimized pipeline for functional network identification. Neuroimage 123, 11–21.
Zerbi, V., Ielacqua, G.D., Markicevic, M., Haberl, M.G., Ellisman, M.H., A, A.B., Frick, A., Rudin, M., Wenderoth, N., 2018. Dysfunctional autism risk genes cause circuit-specific connectivity deficits with distinct developmental trajectories. Cerebr. Cortex 28, 2495–2506.
Zerbi, V., Kleinnijenhuis, M., Fang, X., Jansen, D., Veltien, A., Van Asten, J., Timmer, N., Dederen, P.J., Kiliaan, A.J., Heerschap, A., 2013. Gray and white matter degeneration revealed by diffusion in an Alzheimer mouse model. Neurobiol. Aging 34, 1440–1450.
Zhang, D., Raichle, M.E., 2010. Disease and the brain's dark energy. Nat. Rev. Neurol. 6, 15–28.
Zhang, Y., Bonnan, A., Bony, G., Ferezou, I., Pietropaolo, S., Ginger, M., Sans, N., Rossier, J., Oostra, B., LeMasson, G., Frick, A., 2014. Dendritic channelopathies contribute to neocortical and sensory hyperexcitability in Fmr1(-/y) mice. Nat. Neurosci. 17, 1701–1709.